Int. J. Morphol.,
40(2):507-515, 2022.

Incomplete Petrosphenoidal Foramen: Morphological and Morphometric Analysis and the Proposal of a Classification Study in Brazilian Dry Skulls

Foramen Petrosfenoidal Incompleto: Análisis Morfológico y Morfométrico y Propuesta de Clasificación. Estudio en Cráneos Secos Brasileños

Kennedy Martinez de Oliveira[5]; Severino Denício Gonçalves de Souza[2]; Edson Aparecido Liberti[2]; Gabriel das Chagas Benevenuto[3]; Gustavo Maia de Faria[3]; Ana Clara Ferreira de Almeida[3]; Ana Clara Camillato e Silva[3]; Giuliano Roberto Gonçalves[4]; Yuri Pereira Reis[3]; Walteir Alves Magalhães[1]; Valério Landim de Almeida[1]; Maísa de Fátima Satiro Oliveira[5]; Leandro Henrique Grecco[6]; Arthur Adolfo Nicolato[5] & Fabíola Alves dos Reis[1]

OLIVEIRA, K. M.; SOUZA, S. D. G.; LIBERTI, E. A.; BENEVENUTO, G. C.; FARIA, G. M.; ALMEIDA, A. C. F.; SILVA, A C. C.; GONÇALVES, G. R.; REIS, Y. P.; MAGALHÃES, W. A.; ALMEIDA, V. L.; OLIVEIRA, M. F. S.; GRECCO, L. H.; NICOLATO, A. A. & DOS REIS, F. A. Incomplete petrosphenoidal foramen: Morphological and morphometric analysis and the proposal of a classification. Study in Brazilian dry skulls. *Int. J. Morphol., 40(2)*:507-515, 2022.

SUMMARY: The complete petrosphenoidal foramen, or canal, is an eventual and atavistic bony formation at the boundary between the posterior and middle cranial fossa, by occurrence of ossification of the superior petrosphenoidal ligament. This ligament ossification, which has important clinical and surgical significance, can be complete or incomplete, in variable degrees, and is associated with the passageway of neurovascular structures, such as the abducens nerve and the inferior petrosal sinus. This study, conducted with 175 dry skulls that belong to the University of São Paulo's collection (USP), São Paulo, Brazil, established criteria for a morphological classification of the incomplete petrosphenoid foramen in nine types. In addition, anatomical parameters were established for the morphometric determination of two diameters: the Oblique Diameter (ObDi) and the Maximum Transverse Diameter (MTD). Thus, of the 175 skulls, 146 (83.42 %) presented some of the incomplete forms of the petrosphenoid foramen, and 43 skulls (29.45 %), due to their conservation characteristics, were habilitated to the morphological study, in the classification and in the morphometry (the types I and II of our classification). The type II (incomplete foramen with bony projections of the petrosal tubercle, of the margin of the dorsum of the hypophyseal fossa or of the posterior clinoid process with a distance between them greater than 1mm) and type V (incomplete foramen with a bony projection only in one of the referential structures - posterior clinoid process) were the most common in this study (50 % of the 86 hemiskulls). Morphometry was attributed only to the types: I selar (incomplete foramen with bony projections from the petrosal tubercle and the margin of the dorsum of the hypophyseal fossa with a distance between them less than or equal to 1mm) and to the type II of this classification. The type I selar (9.3 % of the 43 skulls) resulted in an average of 3.25 mm of MTD and 4.63 mm, on average, of ObDi. The type II (25.58 % of the 43 skulls) showed, on average, 4.93 mm of MTD and 7.01 mm of ObDi.

KEY WORDS: Superior petroesphenoidal ligament; Petroesphenoidal foramen; Dorello's Canal; Paraclival triangle.

INTRODUCTION

The skull exhibits a variety of constricted osteofibrous structures that permit the passage of important neurovascular elements through them (Skrzat *et al*., 2017; Oliveira *et al*., 2021). Dorello's canal (DC) is one of these short intracranial passages, seen as an invagination, in part, of the petroclival dura mater at the drainage point of the inferior petrosal sinus

[1] Department of Basic Life Sciences, Federal University of Juiz de Fora, Minas Gerais, Brazil.
[2] Department of Anatomy, Institute of Biomedical Sciences, University of São Paulo, Brazil.
[3] Faculty of Medicine, Federal University of Juiz de Fora, Minas Gerais, Brazil.
[4] School of Medicine, São Leopoldo Mandic, Araras, São Paulo, Brazil.
[5] Faculty of Medicine, Federal University of Minas Gerais, Minas Gerais, Brazil.
[6] São Leopoldo Mandic Institute and Research Center, Campinas, Brazil.

Received: 2021-10-20 Accepted: 2022-02-12

(Wysiadecki *et al*., 2019), delimited superiorly by the superior petroesphenoidal ligament (SPL), also known as petroclinoid, sphenopetrosal, superior petroesphenoidal or Gruber's ligament, laterally by the petrous apex and medially by the lateral margin of clivus' superior part (occipital clivus), constituting part of the inferomedial paraclival triangle (Coquet *et al*., 2018). The DC is responsible for conducting the VI cranial nerve pair (CN VI) - abducens nerve - through the inferior petrosal sinus and the dorsal meningeal branch of the meningohypophyseal trunk until they converge in the cavernous sinus (Bunch, 2016; Reddy *et al*., 2015; Skrzat *et al*.; Pizzolorusso *et al*., 2017a). The knowledge of CD and of SPL is important for the surgical practice, because the CN VI can be injured within the canal in pathological situations, such as craniocerebral trauma (skull base trauma) or intracranial hypertension (Parra *et al*., 2017; Eggerstedt *et al*., 2020; Brown *et al*., 2020). There is also the possibility of compression of the CN VI by the SPL in the hyperextension movement of the brainstem [4], which can result in nerve paralysis / paresis and, consequently, diplopia (Mittal *et al*., 2017). The SPL extends from the petrous apex to the posterior clinoid process, and its ossification can form a osseous bridge, a roof for a variant of the DC, the pestroesphenoidal canal (PC) or petroesphenoidal foramen (PF) (Skrzat *et al*.; Coquet *et al*.; Pizzolorusso *et al*., 2017b; Touska *et al*., 2019). Thus, the anatomoclinical knowledge of these structures is fundamental to prevent and treat injuries that may cause paralysis or paresis of the CN VI (Snyderman *et al*.,2019). The objectives of this work were oriented by the characterization, in dry skulls, of the incomplete petrosphenoidal foramen with the organization of a morphological classification and the anthropometric analyses of two of the nine types of foraminal findings.

MATERIAL AND METHOD

A literature review was conducted in the Medical Literature and Retrieval System Online (PubMed), Excerpta Medica dataBASE (Embase) and Lilacs databases, using the descriptors "Dorello's", "canal" and "petrosphenoidal" and the Boolean operator "AND" to associate the terms among themselves. We included studies published in the last five years that discussed Dorello's canal and/or petrosphenoidal ligament, as well as the transnasal surgical approach involving them, particularly with an anatomical emphasis. As for the specimens, 175 dry skulls were evaluated, belonging to the Human Anatomy Museum "Professor Alfonso Bovero", at the University of São Paulo (USP), Brazil. The specimens were documented with information about age, sex and ethnicity. The analyses were conducted under ambient light, with unarmed vision (without magnifying means) and with the use of morphometric techniques by using a digital pachymeter 150mm/6" (Digimess®), with resolution of 0.01mm/.0005". All the skulls were evaluated bilaterally, by direct cranioscopy and under the perspective of the bone formation of the petrosphenoid foramen, complete or incomplete, considering the microregional integrity at the interfaces of the middle and posterior cranial fossae, and the typical conformation of a natural foramen or a bone structure in incisure (incomplete foramen), in the strict sense of the anatomical practice. In addition, associations of petrosphenoidal foramen with other ossifications such as the caroticoclinoid and interclinoid foramen were identified. The skulls that presented uni or bilateral disjunctions at the level of the petroccipital fissure were not included in this study, as well as the ones with some evidence of fractures and/or abrasions by manipulations. Three referential osseous anatomical elements were necessary for the constitution of the petroesphenoidal incomplete foramen and for the classification proposed in this study - the petrous tubercle, the posterior clinoid process and the margin of the dorsum of the hypophyseal fossa (or sella turcica). Thus, osseous prominences, by partial ossification of the superior petroesphenoidal ligament, related to the referential elements, were the landmarks for establishing the osseous part of the petroesphenoidal foramen. These osseous prominences, indicative of ligament ossification, were considered, for classification and anthropometric measurements, from a minimum length of 0.5 mm. We morphologically classified all findings into nine types, as described in Table I. The table was organized by the authors of this paper and was based on the detailed morphological analysis of the laboratory findings (Fig. 1). Additionally, two measurements were conducted on those findings that were classified as Type I and II - the Maximum Transverse Diameter and the Oblique Diameter (Fig. 2). Types I and II were selected for the morphometric analyses by their narrower osseous conformations, which would approximate to a complete petroesphenoidal foramen with considerable morphological implications for neurosurgical practice. The anatomical parameters for the measurement of the Maximum Transverse Diameter were: posteriorly, from the midpoint between the prominent petrous tubercle (medial to the trigeminal impression) and the petroccipital fissure to the midpoint, anteriorly, between the osseous prominence and the plane of the spheno-occipital synchondrosis. As for the Oblique Diameter, we measured it from the petroccipital fissure to the osseous prominence related to the posterior clinoid process or to the prominence that emerged from the dorsum of the hypophyseal fossa and that was, in this case, the double in length compared to the posterior clinoid process's projection, when concomitants.

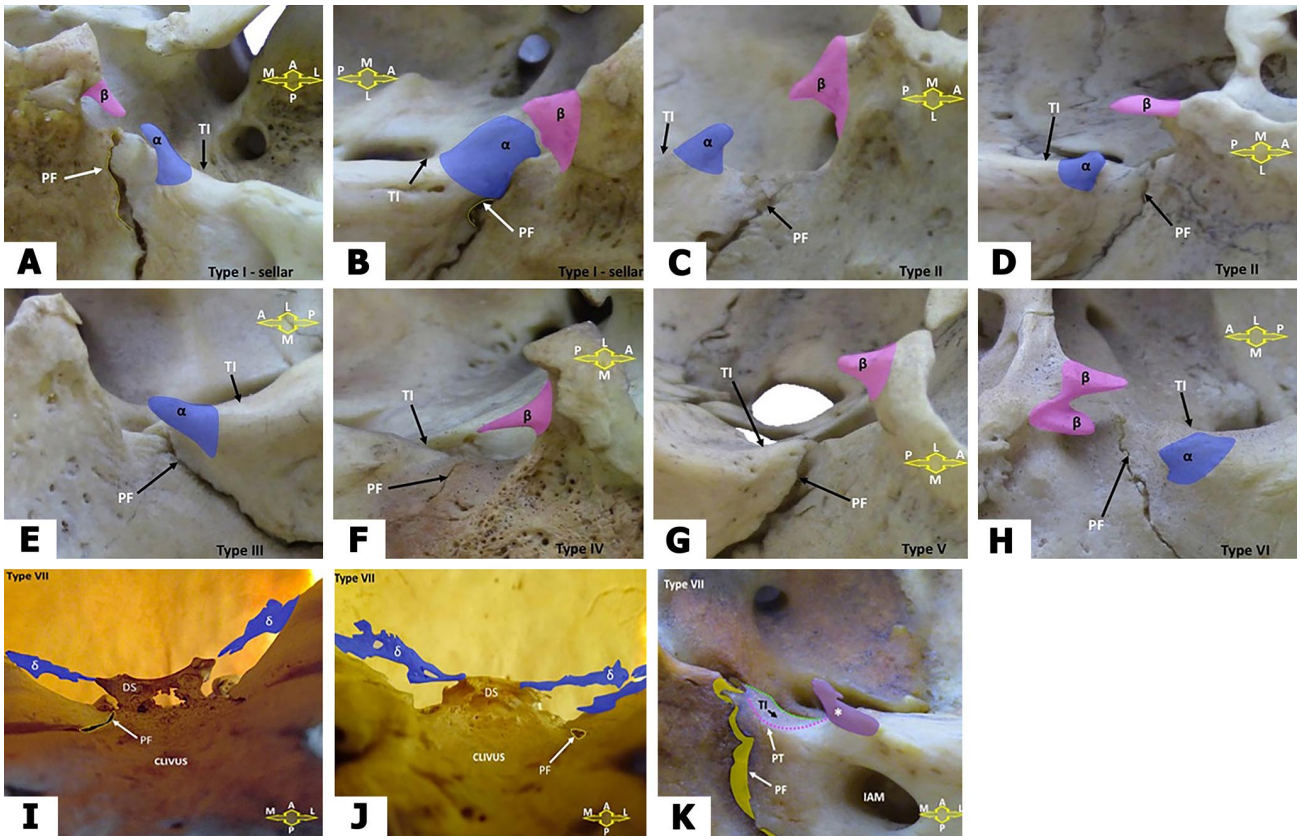

Fig. 1. A-B. Type I sellar: Incomplete foramen with osseous projections from the petrous tubercle and from the dorsal margin of the hypophyseal fossa with a distance between them ≤ 1mm. In 'A' acute or filiform osseous projections and in 'B' the projections are robust laminae. C-D. Type II: Incomplete foramen with osseous projections from the petrous tubercle, from the margin of the dorsum of the hypophyseal fossa or from the posterior clinoid process with a distance between them > 1 mm. In 'C' and 'D', osseous projections with a general triangular pattern. E. Type III: Incomplete foramen with osseous projection, in a triangular pattern, only in one of the referential structures - the petrous tubercle. F. Type IV: Incomplete foramen with osseous projection, in a filiform pattern, only in one of the referential structures - margin of the dorsum of the hypophyseal fossa. G. Type V: Incomplete foramen with osseous projection in only one of the referential structures - posterior clinoid process, in a triangular pattern. H. Type VI: Incomplete foramen with osseous projections on the petrous tubercle and two others - posterior clinoid process and margin of the dorsum of the hypophyseal fossa, in a triangular pattern. A to H abbreviations: PF: petroccipital fissure, TI: indication of trigeminal impression position, a: prominent petrous tubercle, β: prominence of the dorsum of the hypophyseal fossa, A: anterior, P: posterior, M: medial, L: lateral. I-J-K. Type VII: local complex foraminal formations or ossifications not directly related to the petrosphenoidal foramen. In 'I' and 'J', wide laminar ossifications from the posterior margins of the superior petrous sinus to the posterior clinoid process (bilaterally in 'I' and unilaterally in 'J'). In 'K', osseous projection in a triangular pattern (asterisk) positioned lateral to the trigeminal impression (TI). I to K abbreviations: PF: petroccipital fissure, TI: indication of the position of the trigeminal impression, PT: petrous tubercle, DS: dorsum of the hypophyseal fossa, δ: broad ossifications in atypical laminae, IAM: internal acoustic meatus, A: anterior, P: posterior, M: medial and L: lateral.

RESULTS

Of the 175 skulls evaluated, 83.42 % (146 skulls) exhibited some of the types of osseous conformations of the incomplete petrosphenoidal foramen uni or bilaterally and were used to establish the criteria of the current morphological classification. Thus, 29 skulls (16.57 %) exhibited no osseous prominence related to the conformations of the complete or incomplete petrosphenoidal foramen (type 0). Therefore, of the 146 skulls, 43 (29.45 %) were qualified for this study due to their access characteristics, structural preservation, and measurement possibilities for the morphometric evaluations (inclusion criteria). Furthermore, all of those presented, uni or bilaterally, the incomplete forms of the osseous petrosphenoidal foramen. The age of the specimens at the

Table I. Authors' classification for the incomplete forms of the petrosphenoidal osseous foramen.

Classification	Characteristics
Type 0	Absence of osseous projections related to the petrous tubercle, the dorsum of the sella and the posterior clinoid process, concomitantly.
Type I Clinoid	Incomplete foramen with osseous projections of the petrous tubercle and posterior clinoid process with distance between them inferior or equal to 1mm.
Type I Sellar	Incomplete foramen with osseous projections of the petrous tubercle and the margin of the dorsum of the hypophyseal fossa with distance between them inferior or equal to 1mm.
Type II	Incomplete foramen with osseous projections of the petrous tubercle, the margin of the dorsum of the hypophyseal fossa or the posterior clinoid process with a distance between them superior than 1 mm.
Type III	Incomplete foramen with osseous projection in only one of the referential structures - the petrous tubercle.
Type IV	Incomplete foramen with osseous projection in only one of the referential structures - margin of the dorsum of the hypophyseal fossa.
Type V	Incomplete foramen with osseous projection in only one of the referential structures - posterior clinoid process.
Type VI	Incomplete foramen with osseous projections on the petrous tubercle and two others - posterior clinoid process and margin of the dorsum of the hypophyseal fossa.
Type VII	Local complex foraminal formations or ossifications not directly related to the petrosphenoidal foramen.

time of death ranged from 15 to 60 years (mean, 30.4 years), with 33 individuals being male (76.74 %) and 10 female (23.25 %). In 21 specimens (48.8 %), the same morphological type occurred bilaterally, with Types II and V being the most common, representing together 66.6 % of these findings (14:21). In the 22 specimens with distinct morphological occurrences, of which 20 were bilateral and two unilateral, as for the antimere, the predominant type, in the 44 cranial halves combined, was Type V (25.58 %) followed by Types VI, IV and VII, 20.93 %, 18.60 % and 16.27 %, respectively. Considering the antimeres separately, we observed the Type V as the predominant one on the left side (36.36 %) and the Type VI on the right side (31.81 %). Morphometry was applied to the foramina classified as type I (sellar and clinoid) and Type II present together in 34.88 % of the selected skulls, uni or bilaterally. Type I (clinoid) (Table I), foreseen in our study, was not categorized in the selected findings. Thus, we obtained the following results for Type I (sellar) and Type II (Tables II and III). Type I (sellar) occurred in four of the specimens, representing 9.3 % of the 43 skulls selected, and in half, the occurrence was on the left side. Morphometrically, Type I (sellar) demonstrated the Maximum Transverse Diameter (MTD), independent of the antimer, with an average of 3.25 mm (with a minimum finding of 1.41 mm and a maximum of 4.91 mm. While for the Oblique Diameter (ObDi), the average was 4.63 mm, independent of the side - minimum of 2.12 mm and maximum of 8.21 mm. Type II occurred in 11 specimens (25.58 % of the 43 skulls), being bilateral in seven of the findings (16.27 % of the total). Morphometrically, Type II presented, on average, 4.93 mm of MTD, independent of the antimer, with findings from 2.05 mm to 7.29 mm of maximum diameter. As for ObDi, the Type II presented, on average, 7.01 mm in diameter (with a minimum finding of 3.33 mm and a maximum of 10.37 mm) (Table IV). In addition, the study identified, along with the findings of incomplete petrosphenoidal foramen, the caroticoclinoid and/or interclinoid foramen (Fig. 3), which were considered only in their complete osseous conformations. The analyses of the caroticoclinoid and interclinoid foramina were made under the same laboratory conditions described for the petrosphenoidal foramen, but without morphometric evaluations. Thus, in 25.58 % of the specimens (11 out of 43 skulls), these associations were verified, and in 54.54 % of the skulls (six out of 11 specimens) there was a bilateral

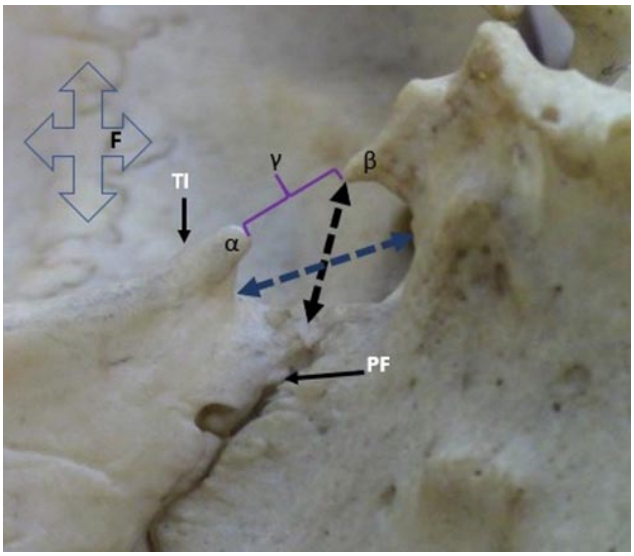

Fig. 2. Indications of diameters in a left hemicranium with the characteristic incomplete petrosphenoidal foramen of Type II. The blue arrow represents the Maximum Transverse Diameter (MTD) and the black arrow the Oblique Diameter (ObDi). PF: petroccipital fissure, TI: indication of the position of the trigeminal impression, α: prominent petrous tubercle, β: prominence of the dorsum of the hypophyseal fossa and γ: the distance between the prominences (in Type II > than 1 mm).

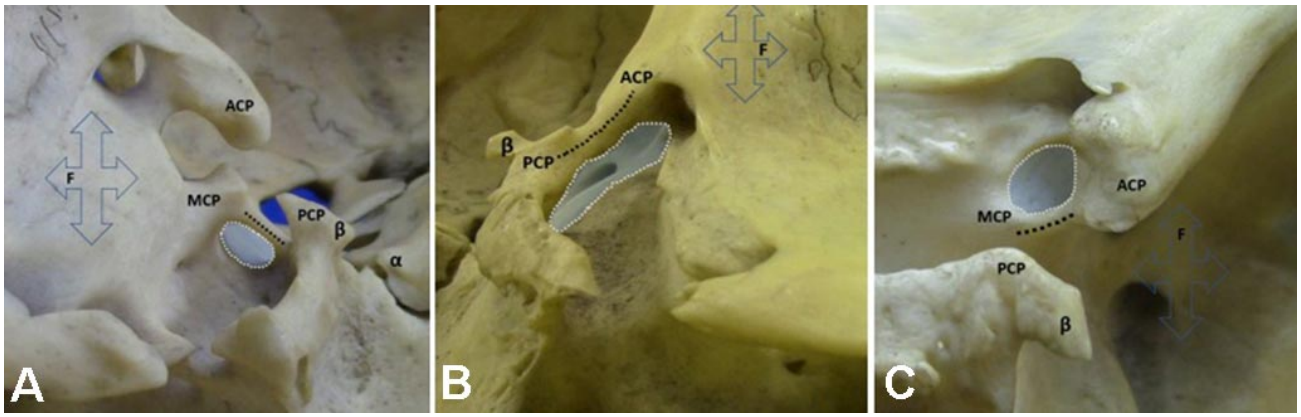

Fig. 3. Findings of complete caroticoclinoid and interclinoid foramina associated with incomplete petrosphenoidal foramina. In 'A' an atypical bilateral "interclinoid" osseous bridge between the medial clinoid process and the dorsal margin of the hypophyseal fossa. In this case, the osseous bridge, due to ossification of the interclinoid ligament, does not extend to the posterior clinoid process. In 'B' a typical interclinoid osseous bridge between the middle and posterior clinoid processes. In 'C' a caroticoclinoid foramen with an osseous bridge, by ossification of the caroticoclinoid ligament. ACP: anterior clinoid process, PCP: posterior clinoid process, MCP: middle clinoid process, α: prominent petrous tubercle, β: prominence associated with the posterior clinoid process and F: frontal.

Table II. Maximum transverse diameter (1) and oblique diameter (2) between the right and left antimers. Type I petrosphenoidal foramen (Sellar).

Skull	Right		Left	
(identification number)	Maximum transverse diameter (1)		Maximum transverse diameter (1)	
	Oblique Diameter (2)		Oblique Diameter (2)	
	1	2	1	2
11	3,53 mm	5,73 mm	4,91 mm	8,21 mm
46	-	-	4,74 mm	4,68 mm
137	1,67 mm	2,42 mm	1,41 mm	2,12 mm

Table III. Maximum transverse diameter (1) and oblique diameter (2) between the right and left antimers of the petrosphenoidal foramen Type II.

Skull	Right		Left	
(identification number)	Maximum transverse diameter (1)		Maximum transverse diameter (1)	
	Oblique Diameter (2)		Oblique Diameter (2)	
	1	2	1	2
24	3,68 mm	7,09 mm	4,94 mm	3,64 mm
25	6,61 mm	9,18 mm	5,08 mm	9,60 mm
46	3,80 mm	3,33 mm	-	-
62	6,12 mm	8,23 mm	4,55 mm	4,68 mm
69	7,29 mm	7,11 mm	6,75 mm	6,50 mm
70	3,18 mm	7,10 mm	3,91 mm	8,23 mm
81	2,05 mm	9,96 mm	5,47 mm	5,03 mm
101	-	-	5,42 mm	10,37 mm
140	-	-	3,20 mm	7,14 mm
154	5,28 mm	7,23 mm	4,43 mm	7,37 mm
177	6,91 mm	4,44 mm	-	-

occurrence, with the caroticoclinoid type in four of the samples and the interclinoid type in two of the samples. As for the unilateral formations, the left side was predominant in 60 % (three of the five sides) with the caroticoclinoid type in three of the five antimers. In five skulls, out of eleven in total, the occurrence of the incomplete petrosphenoidal canal occurred bilaterally in associations with also bilateral formations of the caroticoclinoid and/or interclinoid foramen, with the caroticoclinoid foramen being the most frequent type (three of the five skulls). Thus, of the 22 sides (hemicraniums), the complete caroticoclinoid foramen occurred in 12 (54.54 %) (Table V).

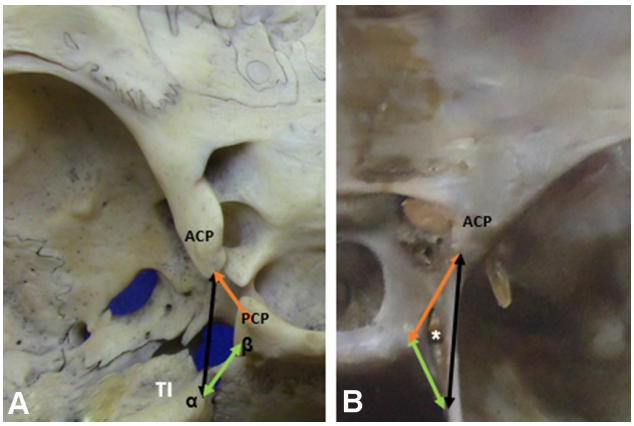

Fig. 4. In 'A' a left hemicranium with the representations of the dispositions of the ligaments: interclinoid (red arrow), petrosphenoidal (green arrow) and the anterior petroclinoid (black arrow). In 'B' a right hemicranium with dura mater and with the arrows tangenting the meningeal folds. Thus, the red arrow indicates the interclinoid fold, related, in depth, to the interclinoid ligament; the green arrow is superimposed on the posterior petroclinoid fold, which is superimposed, in depth, to the petrosphenoidal ligament; the black arrow, superimposed on the anterior petroclinoid fold and the respective ligament, in depth. ACP (anterior clinoid process), PCP (posterior clinoid process). The triangular configuration between the anterior and posterior petroclinoid folds and the interclinoid fold is the oculomotor trigone. Asterisk: oculomotor nerve (III cranial nerve), TI: trigeminal impression, α: prominent petrous tubercle, β: prominence associated with the posterior clinoid process.

Table IV. Maximum transverse diameter and oblique diameter between the Type I (sellar) and the Type II of the petrosphenoidal foramina.

Type	Maximum transverse diameter (average)	Oblique Diameter (average)
I (sellar)	3,25 mm	4,63 mm
II	4,93mm	7,01 mm

DISCUSSION

There is divergence about the first mention in the literature of the CD. Bunch defends that the canal was originally described by the Austrian anatomist Wenzel Leopold Gruber in 1859. In contrast, Parra *et al*. affirm that this osteofibrous canal was described, in detail, only in 1905 by Italian anatomist Primo Dorello (1872-1963) in the work "Considerazioni sopra la causa della paralisi transitoria dell'abducente nelle flogosi dell'orecchio medio", becoming referenced by the eponym "Dorello's canal". The SPL is a fibrous trabeculae, composed of dense collagen fibers under the dura, and is usually located between the petrous apex and the posterior clinoid process (Skrzat *et al*.). In addition, the SPL is an important surgical landmark during subtentorial, transtentorial and transpetrous approaches to the posterior and middle cranial fossae, and its knowledge is a prerequisite for surgeries in its surroundings, such that ossification of the SPL can cause inappropriate interpretation of the anatomy (Parra *et al*.; Touska *et al*.). The SPL is

Table V. Associations of the petrosphenoidal foramina and the caroticoclinoid / interclinoid foramina.

Skull	Bilateral Petrosphenoidal Type	Unilateral Petrosphenoidal Type	Caroticoclinoid or interclinoid foramina	
			Bilateral Type	Unilateral Type
11	I sellar		Caroticoclinoid foramen	
22		Left IV		
		Right 0		Left / Caroticoclinoid
25	II		Interclinoid foramen	
45		Left V		Right / Caroticoclinoid
		Right IV		
62	II			
				Left / Interclinoid
65	V		Interclinoid foramen	
				Left / Caroticoclinoid
69	II		Caroticoclinoid foramen	
115		Left 0	Caroticoclinoid foramen	
		Right VII		
150		Left V		
		Right VII		Right / Caroticoclinoid
161	V			Left / Interclinoid
215	IV		Carotico clinoid foramen	

topographically positioned under the posterior petroclinoid dura mater fold, medially delimiting the oculomotor nerve trigone, as described in Figure 4. In this regard, different variations of the DC and LPS have already been described in the literature, such as their ossification (Skrzat *et al*.). Iwanaga *et al*. (2019) identified, in dissections of 18 specimens (36 sides), the forms of SPL or petroclinoid ligament: simple, duplicated and 'Y' shaped. In addition, the authors reported fixations of these ligaments (of the three forms identified on the dorsum of the pituitary fossa and on the dura mater, in which 5.6 % were ossified (2:36). This mineralization can derive from genetic, metabolic, mechanical stress or atavistic factors (Touska *et al*.). Coquet *et al*. verified a osseous bridge (petrosphenoidal bridge), under the SPL, with the fibrous part of the ligament extending from the middle portion of the osseous bridge to the lateral surface of the clivus. Skrzat *et al*., also reported from dissection an ossified SPL, however partial and limited to the right side. Liu *et al*. (2009) reported petrosphenoid ligament insertions at the margin of the dorsum of the pituitary fossa and also at the posterior clinoid process. This information corroborates with our findings that osseous prominences were observed at the lateral aspect of the dorsum of the pituitary fossa and at the posterior clinoid process. The DC is related to the passage of neurovascular structures, such as the CN VI. However, there is a variation of the passage of the CN VI superior to the SPL when a duplication of the abducens nerve occurs. In this condition, one of the nerve trunks does not follow the pathway commonly associated with DC (Pizzolorusso *et al*., 2017a; Ha?adaj & Skrzat, 2019). According to Mittal *et al*., the abducens nerve, after passing through the canal, after successive passages, reaches the superior orbital fissure, where it will innervate, in the orbit, the lateral rectus extraocular muscle. Thus, Pizzolorusso *et al*. (2017b) report that the course of intracranial NC VI is vulnerable because of its location between neurovascular, ligamentous and osseous structures, and it is potentially injured in various situations, such as cranial hypertension. In addition, DC-related pathologies, such as cavernous sinus aneurysms, intracranial Schwannomas, and chordomas interior to the canal, can compress the NC VI with clinical repercussions (Ha?adaj & Skrzat; Mcdowell *et al*., 2019). However, ossification of the DC and the consequent presence of an osseous foramen can narrow the canal and generate a noncompliant pathway environment surrounding the NC VI, limiting its expansion in conditions of neural inflammation, which can precipitate a condition of NC VI paralysis (Reddy *et al*.; Touska *et al*.). Our study, in dry skulls, did not identify the complete petrosphenoidal foramen, representing complete ossification of the SPL. The detection of SPL variations is also important to avoid damage to the NC VI in endoscopic surgical approaches to access the clivus or in anterior petrosectomy (Coquet *et al*.). In the present study it was evident from the osseous prominences that the SPL can attach to the posterior clinoid process and/or the lateral margin of the dorsum of the sella turcica (pituitary fossa). Touska *et al*., reviewed 240 high resolution non-contrast CT scans of the paranasal sinuses to study ossifications of the skull base, among them of the SPL. The authors identified 10.8 % (26:240) osseous bridges, of which 26.9 % (7:26) were bilateral - 14.3 % (1:7) complete and 85.7 % (6:7) incomplete, and 85.7 % (19:26) unilateral - 26.3 % (5:19) complete and 73.7 % (14:19) incomplete. The thickness and mean area of the ossified ligament was 1.1 mm2 (SD = 0.5 mm^2) and 7.2 mm^2 (SD = 5.5 mm^2), respectively. The authors found that the SPL was the least mineralized among those studied - interclinoid, caroticoclinoid, posterior petroclinoid, pterygospinous and pterygoalar. Iwanaga *et al*. reported SPL thickness between 0.007 mm and 0.49 mm (mean 0.24 mm ± 0.13 mm). The width of the SPL in its narrow part ranged from 0.54 to 3.39 mm (mean 1.49 mm ± 0.61 mm). In this work, the analysis on 146 dried skulls (83.42 % of 175 skulls) detected different configurations of incomplete petrosphenoidal foramen (nine types), as indicated in Table I. The petrosphenoidal foramina were not detected in 16.57 % of our specimens, a number that differs significantly from that found by Touska *et al*., in which only 10.8 % (26:240) of the skulls analyzed contained this osseous bridge. This divergence is probably due to the difference in classification between our study and that of Touska *et al*., given the novelty of our analysis, in addition to the methodological difference in the investigation of the skulls, since they used high-resolution non-contrast CT scans, whereas dry skulls were used in this study. In none of our specimens were detected the complete foraminal formation uni or bilaterally, in addition to the non-detection of Type I Clinoid. However, Type I Clinoid was predicted and identified in skulls that were not included in the 43 specimens selected for the study. As for the osseous structures for morphological definitions and references to morphometries, the petrous tubercle was considered, as described in Iaconetta *et al*. (2001) with or without osseous prominence, and the prominences, by ossifications of the SPL ligament, at the margin of the dorsum of the sella turcica or of the posterior clinoid process. Atypical ossifications in the microregion related to the incomplete petrosphenoidal foramen were observed, associated or not with the osseous prominences references of this study. These formations, sometimes of delicate osseous laminae and in wide extensions, were classified as Type VII, as in Figure 1. The morphometries (Oblique and Maximum Transverse Diameters) were applied to Types: I Selar and II (34.88 % of the 43 skulls) (Tables II and III). The selection of the two types for the adoption of diameters was based on their narrow structures, which reflects the

greatest interest for anatomical and surgical approaches (Fig. 1). The Type I Selar registered, on average, 3.25 mm in Maximum Transverse Diameter (MTD) (minimum 1.41 mm and maximum 4.91 mm) and, on average, 4.63 mm in Oblique Diameter (ObDi) (minimum 2.12 mm and maximum 8.21 mm). The Type II presented, on average, 4.93 mm MTD (minimum 2.05 mm and maximum 7.29 mm) and, on average, 7.01 mm ObDi (minimum 3.33 mm and maximum 10.37 mm) (Table IV). In addition, we found associations in 11 specimens (25.58 % of the 43 skulls) of other formations by ligament ossifications, such as the caroticoclinoid foramen and the interclinoid foramen. The average age in these associations was 31.09 years (with ages ranging from 17 to 60 years), which contrasts with the idea of age-related ligament ossification. Touska *et al*., pointed out a discrete male dominance of ligamentous ossifications at the skull base, which is reflected in our study, since there was a male prevalence, with 33 male skulls (76.74 %) and 10 female skulls (23.25 %) of the incomplete forms of the petrosphenoidal foramen.

CONCLUSION

Ossifications or calcifications of cranial fibrous structures are, by their intimate structural relations, conditions of anatomical relevance and for the various differential diagnoses and surgical approaches. The petrosphenoidal foramina, complete and incomplete, in varying extents, are probably atavistic conditions and related to petroclival neurovascular complexities. In this study, we conducted a detailed analysis of the osseous morphological structures of incomplete petrosphenoidal foramina and obtained a useful classification for these formations. In addition, we characterized, morphometrically, two of the nine types classified in this article.

OLIVEIRA, K. M.; SOUZA, S. D. G.; LIBERTI, E. A.; BENEVENUTO, G. C.; FARIA, G. M.; ALMEIDA, A. C. F.; SILVA, A C. C.; GONÇALVES, G. R.; REIS, Y. P.; MAGALHÃES, W. A.; ALMEIDA, V. L.; OLIVEIRA, M. F. S.; GRECCO, L. H.; NICOLATO, A. A. & DOS REIS, F. A. Foramen petrosfenoidal incompleto: Análisis morfológico y morfométrico y propuesta de clasificación. Estudio en cráneos secos brasileños. *Int. J. Morphol., 40(2)*:507-515, 2022.

RESUMEN: El foramen o canal petroesfenoidal completo es una formación ósea eventual y atávica en el límite entre las fosas craneal posterior y media, por osificación del ligamento petroesfenoidal superior. Esta osificación del ligamento, que tiene un importante significado clínico y quirúrgico, puede ser completa o incompleta, en grados variables, y está asociada al paso de estructuras neurovasculares, como el nervio abducente y el seno petroso inferior. Este estudio se realizó en 175 cráneos secos pertenecientes a la colección de la Universidad de São Paulo (USP), São Paulo, Brasil. Se establecieron criterios para una clasificación morfológica del foramen petrosfenoidal incompleto en nueve tipos. Además, se establecieron parámetros anatómicos para la determinación morfométrica de dos diámetros: el Diámetro Oblicuo (ObDi) y el Diámetro Transversal Máximo (MTD). Así, de los 175 cráneos, 146 (83,42 %) presentaron alguna de las formas incompletas del foramen petrosfenoidal, y 43 cráneos (29,45 %), por sus características de conservación, fueron habilitados para el estudio morfológico, en la clasificación y en la morfometría (los tipos I y II de nuestra clasificación). El Tipo II (foramen incompleto con proyecciones óseas del tubérculo petroso, del margen del dorso de la fosa hipofisaria o del proceso clinoides posterior con una distancia entre ellos mayor de 1 mm) y el Tipo V (foramen incompleto con proyección ósea solamente en una de las estructuras referenciales - proceso clinoides posterior) fueron los más comunes en este estudio (50 % de los 86 hemiscráneos). La morfometría se atribuyó únicamente al Tipo I selar (foramen incompleto con proyecciones óseas desde el tubérculo petroso y el margen del dorso de la fosa hipofisaria con una distancia entre ellos menor o igual a 1mm) y al Tipo II de esta clasificación . El Tipo I selar (9,3 % de los 43 cráneos) resultó en un promedio de 3,25 mm de MTD y 4,63 mm, en promedio, de ObDi. El Tipo II (25,58 % de los 43 cráneos) mostró, en promedio, 4,93 mm de MTD y 7,01 mm de ObDi.

PALABRAS CLAVE: Ligamento petroesfenoidal Superior; Foramen petroesfenoidal; Canal de Dorello; Triángulo paraclival.

REFERENCES

Brown, D.; McConnell, N.; List, R.; Olubajo, F.; Highley, R.; Storey, M. & Kounin, G. Spontaneous haemorrhage into a large abducens nerve schwannoma: a case report. *Br. J. Neurosurg., 34(2)*:224-6, 2020.

Bunch, P. M. Anatomic eponyms in neuroradiology: head and neck. *Acad Radiol., 23(10)*:1319-32, 2016.

Coquet, T.; Lefranc, M.; Chenin, L.; Foulon, P.; Havet, É. & Peltier, J. Unilateral duplicated abducens nerve coursing through both the sphenopetroclival venous gulf and cavernous sinus: a case report. *Surg. Radiol. Anat., 40(7)*:835-40, 2018.

Eggerstedt, M.; Dua, S. G.; Varelas, A. N.; Bhabad, S. H.; Batra, P. S. & Tajudeen, B. A. Enlargement of Dorello's canal as a novel radiographic marker of idiopathic intracranial hypertension. *J. Neurol. Surg. B Skull Base, 81(3)*:232-6, 2020.

Ha?adaj, R. & Skrzat, J. Bilateral duplication of the abducens nerve - case study. *Folia Med. Cracov., 59(4)*:13-20, 2019.

Iaconetta, G.; Tessitore, E. & Samii, M. Duplicated abducent nerve and its course: microanatomical study and surgery-related considerations. *J. Neurosurg., 95(5)*:853-8, 2001.

Iwanaga, J.; Altafulla, J. J.; Gutierrez, S.; Dupont, G.; Watanabe, K.; Litvack, Z. & Tubbs, R. S. The petroclinoid ligament: its morphometrics, relationships, variations, and suggestion for new terminology. *J. Neurol. Surg. B Skull Base, 81(6)*:603-9, 2019.

Liu, X. D.; Xu, Q. W.; Che, X. M. & Mao, R. L. Anatomy of the petrosphenoidal and petrolingual ligaments at the petrous apex. *Clin. Anat., 22(3)*:302-6, 2009.

Mcdowell, M. M.; Whelan, R.; Goldschmidt, E.; Venteicher, A. S.; Snyderman, C.; Fernandez-Miranda, J. C.; Gardner, P. A. & Wang, E. W. Predictors of improved abducens nerve palsy following endoscopic endonasal approach to skull base lesions. *J. Neurol. Surg. B Skull Base, 80(S. 01)*:S1-S244, 2019.

Mittal, S. O.; Siddiqui, J. & Katirji, B. Abducens nerve palsy due to inferior petrosal sinus thrombosis. *J. Clin. Neurosci., 40*:69-71, 2017.

Oliveira, K. M.; De Almeida, V. L.; López, C. A. C.; Brandão, G. T.; Trancoso, M. G. B., Oliveira, M. F. S.; Morais, I. C. L., Soares, D. C. B. & Costa, L. C. M. The pterygospinous foramen (civinini) and the pterygoalar (Crotaphiticobuccinatorius) Laboratory findings. *Int. J. Morphol., 39(1)*:198-204, 2021.

Parra, J. E. D.; Rios, J. B. & Zuluaga, J. M. Dorello's Canal or Abducens Nerve Canal: Constancy or Inconstancy?. *Int. J. Morphol., 35(1)*:233-6, 2017.

Pizzolorusso, F.; Cirotti, A. & Pizzolorusso, G. Anatomic variation of the abducens nerve in a single cadaver dissection: the "petrobasilar canal." *Acta Neurochir. (Wien), 159(4)*:677-80, 2017a.

Pizzolorusso, F.; Cirotti, A. & Pizzolorusso, G. Petrobasilar, petroclival, or petrosphenoidal canal of the abducens nerve. *Acta Neurochir. (Wien), 159(11)*:2147-8, 2017b.

Reddy, R. K.; Reddy, R. K.; Jyung, R. W.; Eloy, J. A. & Liu, J. K. Gruber, Gradenigo, Dorello, and Vail: key personalities in the historical evolution and modern-day understanding of Dorello's canal. *J. Neurosurg., 124(1)*:224-33, 2015.

Skrzat, J.; Mróz, I.; Spulber, A.; Zarzecki, M. & Walocha, J. Ossification of the petrosphenoid ligament - a case study. *Folia Med. Cracov., 57(2)*:87-94, 2017.

Snyderman, C. H.; Gardner, P. A. & Tyler-Kabara, E. C. Surgical management of clival chordomas in children. Oper. Tech. Otolaryngol. *Head Neck Surg., 30(1)*:6372, 2019.

Touska, P.; Hasso, S.; Oztek, A.; Chinaka, F. & Connor, S. E. J. Skull base ligamentous mineralisation: evaluation using computed tomography and a review of the clinical relevance. *Insights Imaging, 10*:55, 2019.

Wysiadecki, G.; Ha?adaj, R.; Polguj, M.; Z˙ytkowski, A. & Topol, M. Bilateral extensive ossification of the posterior petroclinoid ligament: an anatomical case report and literature review. *J. Neurol. Surg. A Cent. Eur. Neurosurg., 80(2)*:122-6, 2019.

Corresponding author:
Kennedy Martinez de Oliveira
Anatomy and Image Department
Federal University of Minas Gerais - UFMG
Av. Professor Alfredo Balena, 190
Belo Horizonte
Zip Code 30130-100
Minas Gerais
BRAZIL

E-mail: kennedymartinez@ufmg.br